International Journal of Mechatronics, Electrical and Computer Technology

Vol. 4(12), Jul, 2014, pp. 1353-1365, **ISSN**: 2305-0543
Available online at: http://www.aeuso.org

Comparison of Different Permanent Magnet Arrangements of BLDC Motors based on Finite Element Analysis

Hossein Asgharpour-Alamdari[1*], Hamidreza Izadfar[1], Reza Ilka[1], Yousef Alinejad-Beromi[1], Hamid Yaghobi[1]

[1]Iran,Semnan, Semnan University, Department of Electrical Engineering

Corresponding Author: Hossein Asgharpour-Alamdari

*Corresponding Author's E-mail: *Asgharpour.alamdari@gmail.com*

Abstract

This paper presents a comparison of different permanent magnet arrangement of brushless DC motor. Firstly, design and principal equations of these motors are provided. Five common permanent magnet arrangements are considered. Best arrangement is selected in terms of performance characteristics such as efficiency, output torque, weight of motor and PMs and etc. based on simulation with finite element analysis. Simulation is conducted by 2-D finite element analysis software.

Keywords: Brushless Motor, Permanent Magnet, Finite Element Analysis, Maxwell Software

1. Introduction

Among all types of electrical motors, DC motors are highly efficient and suitable to be used as servomotors. However, they need brushes and a commutator which require maintenance. When functions of the commutator and brushes were implemented by solid-state switches, maintenance-free motors were realized. These motors are now known as brushless DC motors [1-3]. In addition, permanent magnet motors are increasingly used in so many applications due to simpler design procedure, higher efficiency (lower loss) and power density and minimum volume. Brushless Permanent Magnet (PM) motors are widely used in telecommunications, electronics, and industrial equipment applications [3]. In this paper, an inner brushless motor is considered. This type of construction has more popularity among brushless motors. Because the windings remain stationary, no potentially troublesome moving electrical contacts, i.e., brushes are required. In addition, stationary windings are easier to keep cool [4]. Main advantages of the BLDC motors are

International Journal of Mechatronics, Electrical and Computer Technology

Vol. 4(12), Jul, 2014, pp. 1353-1365, **ISSN**: 2305-0543
Available online at: http://www.aeuso.org

high efficiency, low maintenance and long life, low noise, control simplicity, low weight, and compact construction. On the other hand, the main disadvantages of the BLDC motors are high cost of the permanent magnet materials, the problem of demagnetization, and limited extended speed, constant power range (compared to a switched reluctance machine) [5, 8]. Few investigations on different magnet topologies are reported in the literature. For instance, Stumberger et al. [4] have proposed Comparison of torque capability of three-phase permanent magnet synchronous motors (PMSM) with different permanent magnet arrangement. This paper determines which arrangement has better performance according to their torque capability. However, there is a lack of work performing on comparison of different permanent magnet topologies of BLDC motors. In this paper, authors try to cover this gap. This paper aims to determine the capabilities of different permanent magnet arrangements of BLDC motor. For this purpose, five different permanent magnet topologies are considered. Then, finite element analysis is employed to determine performance characteristic of different magnet arrangements.

2. Design Equations

In the design equations that follow, the approach is to start with basic motor geometrical constraints and a magnetic circuit description of flux flow. The considered topology is shown in Fig.1.

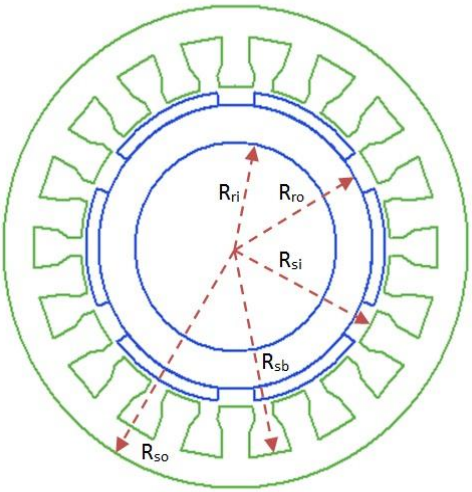

Figure 1: Motor topology showing geometrical definitions

International Journal of Mechatronics, Electrical and Computer Technology
Vol. 4(12), Jul, 2014, pp. 1353-1365, **ISSN**: 2305-0543
Available online at: http://www.aeuso.org

The flux from each magnet, which is coupled to the adjacent magnets, splits equally in both the stator and rotor back irons. Thus, the back-iron flux is one-half of the air gap flux:

$$\phi_{bi} = \frac{\phi_g}{2} \tag{1}$$

Considering the maximum flux density allowed in the back iron as B_{max} from the table of fixed values, form Eq. (11) the back-iron width must be:

$$w_{bi} = \frac{\phi_g}{2 B_{max} K_{st} L} \tag{2}$$

Where, K_{st} is the lamination-stacking factor.

Since there are $N_{sm} = N_{spp} / N_{ph}$ slots and teeth per magnet pole, the air gap flux from each magnet travels through N_{sm} teeth. Therefore, each tooth must carry $1/N_{sm}$ of the air gap flux. If the maximum flux density allowed in the teeth is also B_{max}, the required tooth width is

$$w_{tb} = \frac{2}{N_{sm}} w_{bi} \tag{3}$$

Using Eq. (1) and Eq. (2), all geometric parameters are obtained.

The PM length L_{PM} can be calculated as

$$L_{PM} = \frac{\mu_r B_g}{B_r - \left(\frac{K_f}{K_d} B_g\right)} K_c g \tag{4}$$

Where, μ_r is the recoil relative permeability of the magnet, B_r is the residual flux density of the PM material, K_d is the leakage flux factor, K_c is the Carter factor, $K_f = B_{gpk}/B_g$ is the peak value corrected factor of air gap flux density in the motor. These factors can be obtained using FEM analysis [7, 8]. Given the relationship between torque and the other motor parameters,the electrical parameters can be found. The torque developed by a single phase when $N_{spp} = 1$ is:

$$T = (2 N_{ph} B_g L I) R_{ro} \tag{5}$$

International Journal of Mechatronics, Electrical and Computer Technology
Vol. 4(12), Jul, 2014, pp. 1353-1365, **ISSN**: 2305-0543
Available online at: http://www.aeuso.org

Where the product in parentheses is the force produced by the interaction of N_m magnet poles providing air gap flux density (B_g), with each pole interacting with n_s conductors each carrying a current i exposed to B_g over a length L. In this situation, where there may be more than one slot per pole per phase, n_s must be replaced by the number of turns per pole per phase $n_{tpp} = N_{spp}n_s$, which gives a torque expression of

$$T = N_m B_g L I R_{ro} N_{spp} n_s \tag{6}$$

If $N_{spp} > 1$, the air gap flux density must be modified by the distribution factor and pitch factor. Moreover, if the magnets are skewed, the skew factor given in Eq. (7) must be included.

$$K_s = 1 - \frac{\theta_{se}}{2\pi} \tag{7}$$

Inclusion of these terms gives a final torque expression of

$$T = N_m K_w K_s B_g L I R_{ro} N_{spp} n_s \tag{8}$$

Now, using Eq. (8) and the input-output power relationship $T.\omega = e_b .i$, the peak counter-emf at rated speed ω_m is

$$E_{max} = \frac{T.\omega_m}{I} = 2N_{ph} B_g L \omega_m R_{ro} K_p K_d K_s \tag{9}$$

3. Analysis Method and Selecting the Best Design: Procedure, Results and Discussion

Motor description is shown in Table1. These ratings are chosen because voltage, power and speed of this table are very common in too many applications. This motor has been used with five different permanent magnet arrangements. Fig.2 shows different magnet layouts and the selected motor is simulated in each stage with one of these arrangements, separately. In Fig.2, topologies a, b and c are surface-mounted permanent magnets (SMPM) while topologies d and e are interior permanent magnets (IPM). In the surface-mounted machine, the air gap might be non-uniform, while for the interior mounted machine, the air gap is uniform. In the

Vol. 4(12), Jul, 2014, pp. 1353-1365, **ISSN**: 2305-0543
Available online at: http://www.aeuso.org

case of rotor-surface-mounted permanent magnets, a permanent magnet machine is, in principle, of the nonsalient-pole type. In the case of interior magnets instead, the rotor is a salient-pole construction. Fig.2.a is a traditional radial arc magnet shape. Fig.2.b is similar, except the sides of the magnet are parallel, rather than radial. Another topology is shown in Fig.2.c, where the sides are parallel and the bottom is flat. The rotor shown in Fig.2.d is known as the spoke configuration. This configuration promotes flux concentration because the magnet surface area is greater than the rotor surface area. This rotor type is useful for gaining better performance from ferrite magnet material and has the benefit of using rectangular block magnets. The final rotor shown in Fig.3.e, has buried magnets. This construction is beneficial for high speed operation, since the rectangular magnets are entirely enclosed in a solid rotor structure. While the interior permanent magnet rotors support the use of rectangular magnets, the presence of ferromagnetic material at the rotor surface dramatically increases the air gap inductance. Furthermore, it adds a reluctance component to the torque produced [4].

TABLE: 1 Motor Description

Design Parameters	Value
Voltage	220 V
Output power	550 W
Number of poles	4
Number of slots	24
Rated Speed	1500 rpm

International Journal of Mechatronics, Electrical and Computer Technology
Vol. 4(12), Jul, 2014, pp. 1353-1365, **ISSN**: 2305-0543
Available online at: http://www.aeuso.org

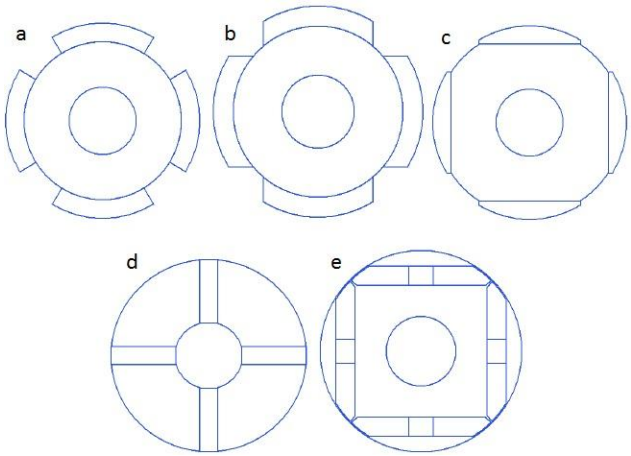

Figure 2: Five different permanent magnet topologies

The material used for stator and rotor core is Steel M19 and magnets are NdFeB with residual flux density of 1.2 T. NdFeB magnets offer the highest energy density at reasonable costs. Their major drawback, compared to SmCo, is temperature sensitivity. When using NdFeB magnets, the motor's temperature must be kept below 170–250°. Since the rotor losses are small, passive cooling is employed for the rotor [6, 7]. Simulation is done with Maxwell software which is based on finite element analysis (FEA). Maxwell is one of the most famous and reliable software in design and analysis of electrical machines.

4. Comparison Procedure

Comparison of different arrangements has been done in terms of output torque, efficiency, cogging torque, motor weight and flux density of the motor. Fig.3 shows air gap flux density for five different arrangements. As shown arrangement c has a similar behaviour to a sinusoidal wave. Arrangements a, b, d and e are more trapezoidal. Generally speaking, air gap flux density of BLDC motors is trapezoidal. It can be inferred that, when PMs are skewed (as configuration c), the air gap would be more uniform and hence flux density in the air gap would be distributed more smoothly. Therefore, back-EMF will have a more sinusoidal shape. Fig.4 shows five different arrangements efficiency versus speed. Arrangements a, b and c are alike but, for arrangements d and e

International Journal of Mechatronics, Electrical and Computer Technology

Vol. 4(12), Jul, 2014, pp. 1353-1365, **ISSN**: 2305-0543
Available online at: http://www.aeuso.org

there is deformity from common plots which is because of its magnet shape. Again arrangement c has better characteristic than the other ones. Fig.5 shows output torque versus speed. Fig.6 shows cogging torque. Fig.7 shows flux lines and flux density distribution. Table 2 shows motor's crucial characteristics for five permanent magnet arrangements.

TABLE: 2 Simulation results

	Surface1	Surface2	Surface3	Interior1	Interior2
Efficiency %	87.2	87.2	87.85	87.09	84.79
T-rated (N.m)	3.42	3.35	3.75	2.49	4.02
Net Weight (kg)	5.06	5.08	5.27	5.13	4.97
T-Cogging (N.m)	0.665	0.6	0.497	0.25	0.47
I-rms (A)	2.45	2.45	1.38	2.498	2.57

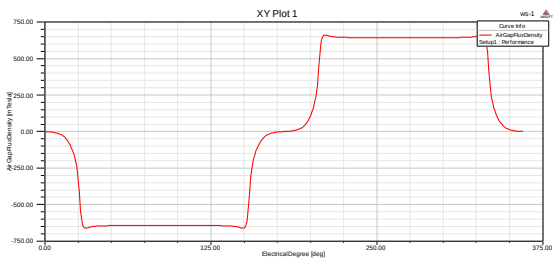

(a)

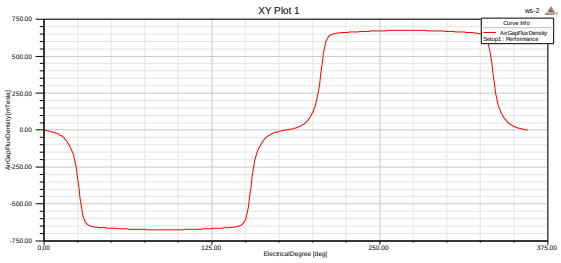

(b)

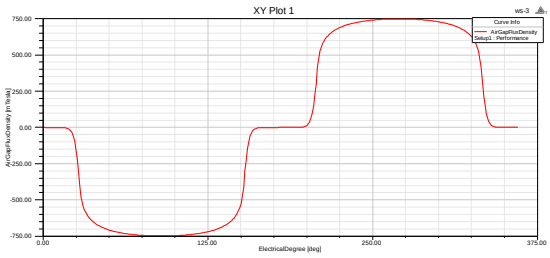

(c)

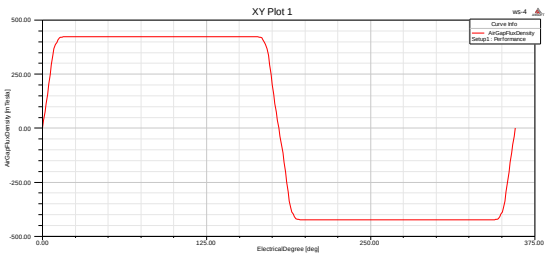

(d)

International Journal of Mechatronics, Electrical and Computer Technology

Vol. 4(12), Jul, 2014, pp. 1353-1365, **ISSN**: 2305-0543

Available online at: http://www.aeuso.org

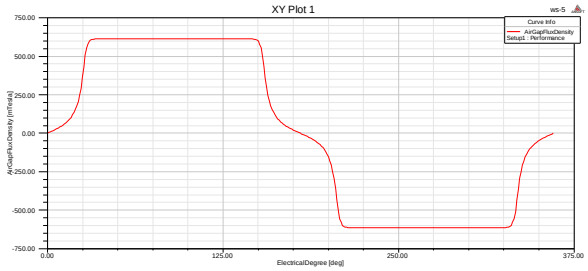

(e)

Figure 3: Air gap flux density of different permanent magnet arrangements

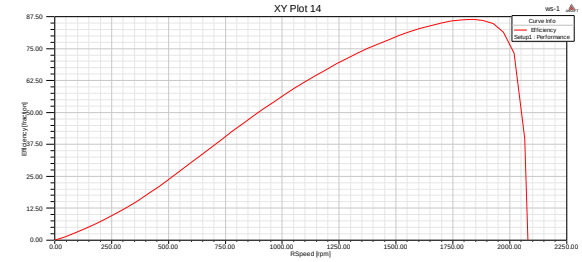

(a)

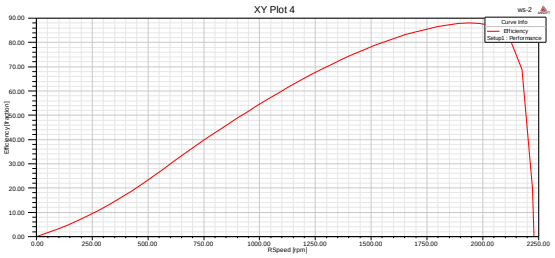

(b)

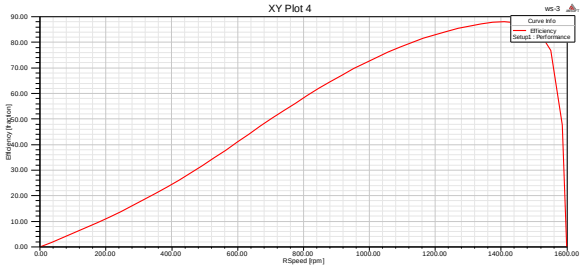

(c)

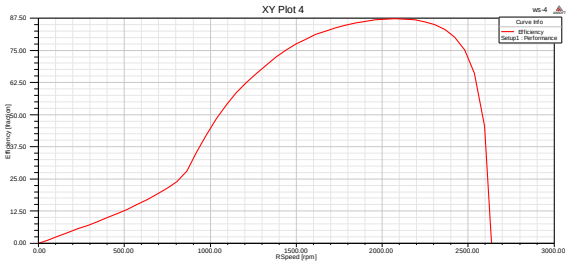

(d)

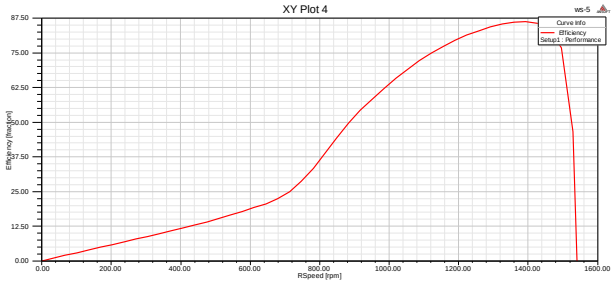

(e)

Figure 4: efficiency versus speed of different permanent magnet arrangements

International Journal of Mechatronics, Electrical and Computer Technology

Vol. 4(12), Jul, 2014, pp. 1353-1365, **ISSN**: 2305-0543

Available online at: http://www.aeuso.org

(a)

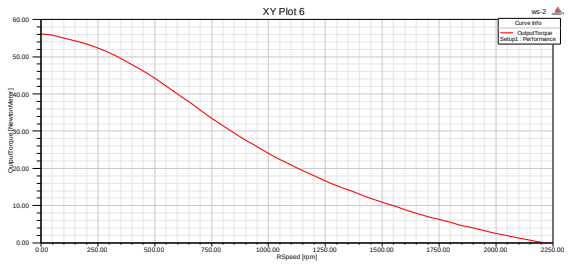

(b)

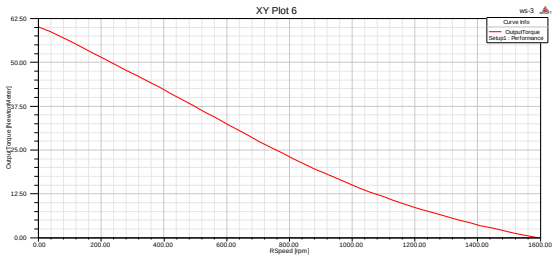

(c)

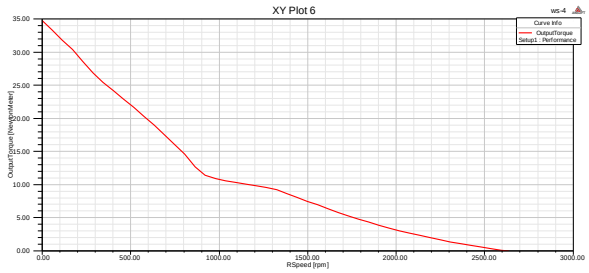

(d)

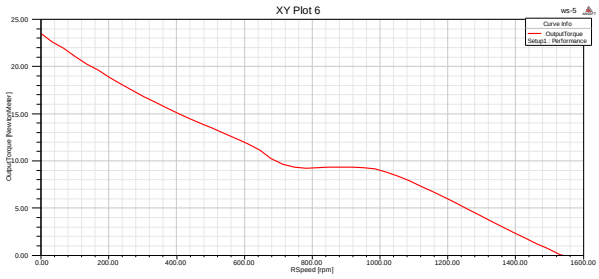

(e)

Figure 5: Output torque versus speed of different permanent magnet arrangements

Power density and torque density are the measures to judge how the active materials of a BLDC motor are best utilized. Torque is depended on some parameters. Torque is increase by increasing the number of poles and also increasing main dimensions of motor i.e. motor axial length and outside rotor radius, while increasing these parameters are always restricted due to economical constraints.

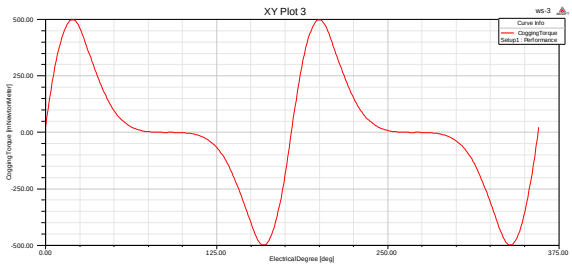

(a)

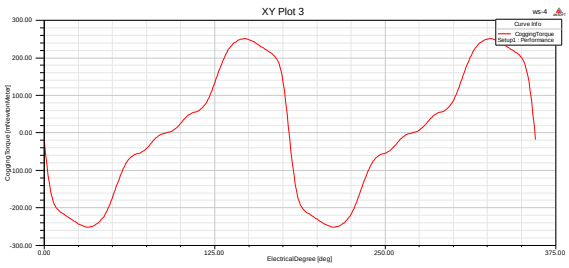

(b)

International Journal of Mechatronics, Electrical and Computer Technology

Vol. 4(12), Jul, 2014, pp. 1353-1365, **ISSN**: 2305-0543
Available online at: http://www.aeuso.org

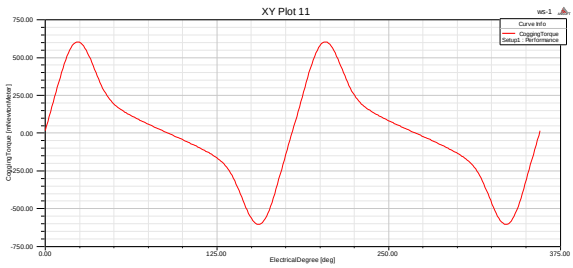

(c)

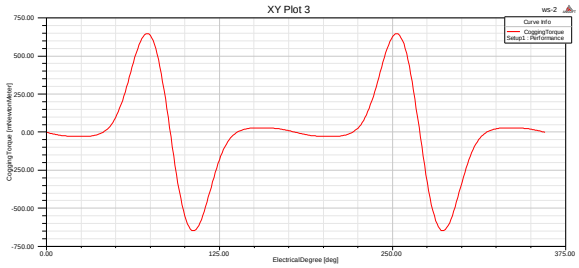

(d)

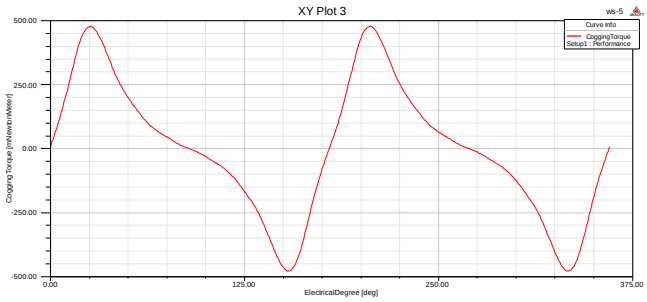

(e)

Figure 6: cogging torque of different permanent magnet arrangements

Cogging torque describes the interaction of the rotor magnets acting on the stator teeth or poles independent of any current. While this torque is often considered beneficial in step motors, it is considered detrimental in brushless permanent magnet motors [4]. Cogging torque is decreased by increasing the number of poles, teeth and phase of the motor. Generally, cogging torque can be reduced employing a fractional-pitch winding, which is used in many applications, particularly odd stator slots. A method to eliminate the cogging torque in BLDC machines is to eliminate its source: the reluctance changes in the magnetic circuit during the rotation of the PM around the stator. In a traditional brushless motor, copper wires are wound through slots in a laminated steel core. As magnets pass by the lamination shoes, they have a greater attraction to the iron at the top of the laminations than to the air gap between shoes. This uneven magnetic pull causes cogging, which in turn increases motor vibrations and noise. Therefore, the key to smooth brushless performance centers on a slotless stator. Additionally, a slotless design significantly reduces damping losses [5, 8]. From a point of view, one can say a motor with less effective value of cogging torque has better performance. As shown in Fig.6, arrangement d has lower cogging rather than others.

International Journal of Mechatronics, Electrical and Computer Technology

Vol. 4(12), Jul, 2014, pp. 1353-1365, **ISSN**: 2305-0543

Available online at: http://www.aeuso.org

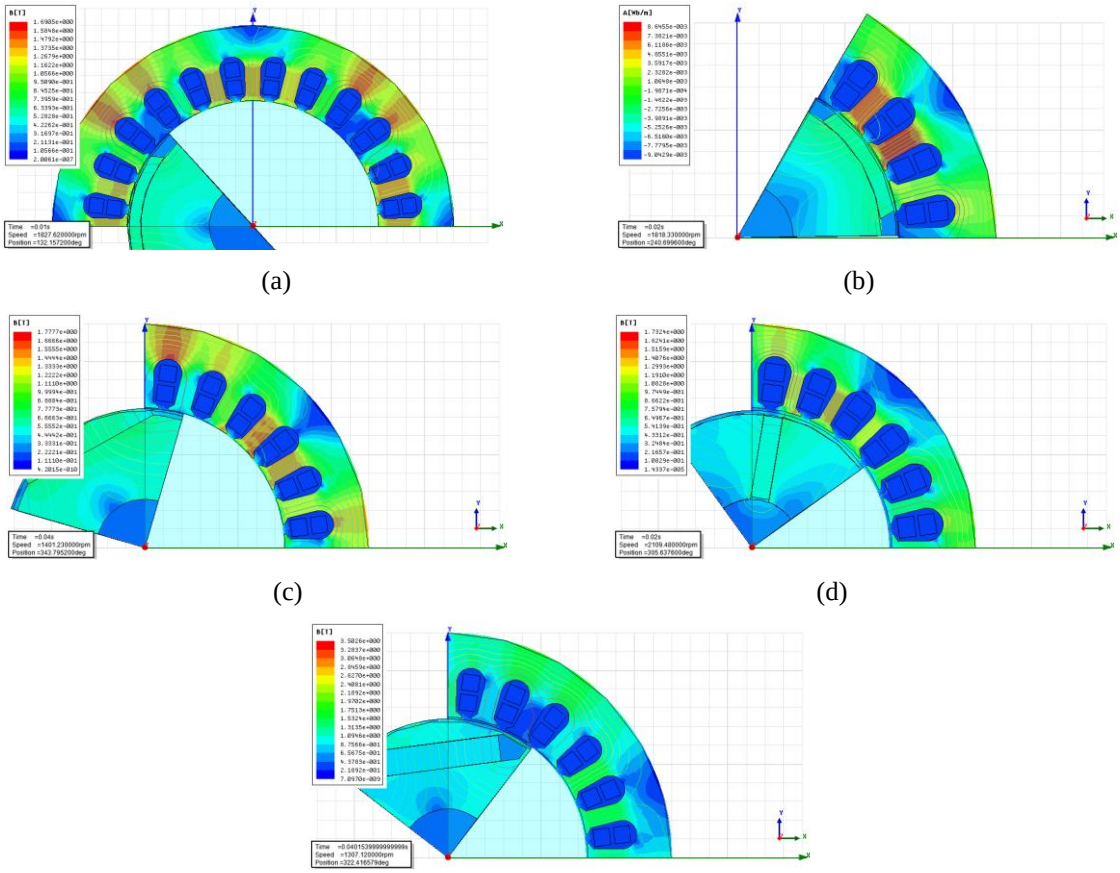

(a) (b) (c) (d) (e)

Figure 7: flux lines and flux density distribution of different permanent magnet arrangements

Vol. 4(12), Jul, 2014, pp. 1353-1365, **ISSN**: 2305-0543
Available online at: http://www.aeuso.org

Conclusion

In this paper a comparison between different rotor types of brushless DC motor was presented. For this purpose, at first the relationships were expressed. The best rotor configuration was selected from 5 different types based on their performance characteristics such as efficiency, output torque, the motor weight, rated current and cogging torque. Finally, it was found that the topology C has the best general performance. Of course it could be cited that each topologies has good performance characteristics that are preferred based on the application for each of them.

References

[1] A. Hughes, "Electric Motors and Drives", Newnes; 3rd edition, 2005.

[2] W. Yeadon, A. Yeadon, Handbook of Small Electric Motors. McGraw-Hill Professional; 1 edition, 2001.

[3] J.R. Hendershot, T.J.E. Miller, Design of Brushless Permanent-Magnet Machines. Motor Design Books LLC: Second Edition, 2010.

[4] D. C. Hanselman, Brushless permanent magnet motor design, Magna Physics Publishing, 2nd edition, 2006.

[5] J. F. Gieras, M. Wing, Permanent Magnet Motor Technology: Design and Applications, CRC Press, 2nd edition, 2002.

[6] H. A. Toliyat, G. B. Kilman, Handbook of Electric Motors, CRC Press, 2nd Edition, 2004.

[7] E. S. Hamdi, Design of Small Electrical Machines, John Wiley & Sons, 1994.

[8] J. Pyrhonen, T. Jokinen and V. Hrabovcova, Design of Rotating Electrical Machines, John Wiley & Sons, 2008.

[9] B. Stumberger, G. Stumberger, M. Hadziselimovi, A. Hamler, V. Gorican, M. Yesenik and M. Trlep, Comparison of torque capability of three-phase permanent magnet synchronous motors with different permanent magnet arrangement, Journal of Magnetism and Magnetic Materials 316 (2007) e261–e264.

International Journal of Mechatronics, Electrical and Computer Technology

Vol. 4(12), Jul, 2014, pp. 1353-1365, **ISSN**: 2305-0543

Available online at: http://www.aeuso.org

Authors

Hossein Asgharpour-Alamdari is currently pursuing his PhD degree in power electrical engineering in Semnan University. His research interests include winding design of electrical machines.

Hamidreza Izadfar is currently an Assistant Professor with the Electrical and Computer Department, Semnan University, Semnan, Iran. His research interests include analysis of electrical machines.

Reza Ilka was born in Ghaemshahr, Iran, in 1988. He received B.Sc and M.Sc degree in power electrical engineering from Babol University of Technology, Iran in 2010 and 2012, respectively. He is currently pursuing his PhD degree in power electrical engineering in Semnan University. His research interests include design and optimization of electrical machines.

Yousef Alinejad-Beromi received his degree in electrical engineering from K.N.T. University, Tehran-Iran and his M.Sc. and Ph.D. from U.W.C.C., Cardiff, U.K. in 1989 and 1992, respectively. He is currently an Assistant Professor with the Electrical and Computer Department, Semnan University, Semnan, Iran. His research interests include analysis and investigation of electric machines, magnetic materials and magnetism.

Hamid Yaghobi is currently an Assistant Professor with the Electrical and Computer Department, Semnan University, Semnan, Iran. His research interests include analysis and design of electrical machines specifically faults detection issues of electrical machines.